Published online 14 December 2006 *Nucleic Acids Research, 2007, Vol. 35, No. 2* ***353–362***
doi:10.1093/nar/gkl1027

Role of Elg1 protein in double strand break repair

Hideaki Ogiwara[1], Ayako Ui[1], Takemi Enomoto[1,2] and Masayuki Seki[1,*]

[1]Molecular Cell Biology Laboratory, Graduate School of Pharmaceutical Sciences, Tohoku University, Aoba 6-3, Aramaki, Aoba-ku, Sendai 980-8578, Japan and [2]Tohoku University 21st Century COE Program 'Comprehensive Research and Education Center for Planning of Drug development and Clinical Evaluation', Sendai, Miyagi 980-88578, Japan

Received September 25, 2006; Revised and Accepted November 15, 2006

ABSTRACT

The inaccurate repair of DNA double-strand breaks (DSBs) can result in genomic instability, and additionally cell death or the development of cancer. Elg1, which forms an alternative RFC-like complex with RFC2-5, is required for the maintenance of genome stability in *Saccharomyces cerevisiae,* and its function has been linked to DNA replication or damage checkpoint response. Here, we show that Elg1 is involved in homologous recombination (HR)-mediated DSB repair. Mutants of *elg1* were partially defective in HR induced by methylmethanesufonate (MMS) and phleomycin. Deletion of *ELG1* resulted in less efficient repair of phleomycin-induced DSBs in G_2/M phase-arrested cells. During HR between *MAT* and *HML* loci, Elg1 associated with both the *MAT* locus near the HO endonuclease-induced DSB site, and the *HML* homologous donor locus. The association of Elg1 with the *MAT* locus was not dependent on Rad52. However, Elg1 association with the *HML* locus depended on Rad52. Importantly, we found that two of the later steps in HR-mediated repair of an HO endonuclease-induced DSB, primer extension after strand invasion and ligation, were less efficient in *elg1* mutants. Our results suggest that Elg1 is involved in DSB repair by HR.

INTRODUCTION

Many overlapping mechanisms of genome surveillance and DNA repair reside in eukaryotic cells to ensure genome stability. Genomic instability, which occurs in normal cells at a low rate, is enhanced in cancer cells. Among the signs of genome instability observed in many cancer cells are elevated mutation rates, and gross chromosomal rearrangements, such as deletions and translocations (1). The yeast *Saccharomyces cerevisiae*, a simple eukaryote, is a useful model system for studying genome stability, because the basic repair pathways in yeast, and the regulatory mechanisms that control them, are well conserved across species. Elg1 (enhanced level of genome instability) was identified in *S.cerevisiae* as a genome stabilizer, and its human counterpart has also been identified (2–4). Elg1 exhibits sequence similarity to one of the five subunits of the replication factor C (RFC) complex, Rfc1, and replaces this subunit in the RFC complex. For this reason, Elg1-containing RFCs are called alternative RFCs.

RFC was originally identified as a protein complex required for SV40 DNA replication *in vitro*, and consists of five different subunits (RFC1-5 in humans) (5,6). During DNA replication, the classical RFC complex recognizes primer termini, and catalyzes loading of the sliding clamp, which includes proliferating cell nuclear antigen (PCNA), onto the DNA, not RNA (7,8). PCNA remains associated with the DNA, and acts as a processivity factor for DNA polymerase δ on either the lagging and/or leading DNA strand. At least three alternative forms of the RFC, including the Elg1-containing complex, have been identified recently in yeast and humans (2–4). The Rad24–Rfc2-5 complex, in which Rfc1 is replaced by Rad24 (9), loads a PCNA-like heterotrimer clamp, consisting of Rad17, Ddc1 and Mec3, onto the DNA (3,10). Both the Rad24/Rfc2-5 clamp loader and the Rad17/Ddc1/Mec3 clamp are required for activation of the DNA damage checkpoint in G_1 and G_2, and contribute to S phase checkpoint regulation. A third Rfc1-like protein, Ctf18, replaces Rfc1 the Ctf18–Rfc2-5 complex (11–13). Ctf18/Rfc2-5 contains two additional subunits, Ctf8 and Dcc1, and mutations in any of these three proteins, *ctf18*, *ctf8*, or *dcc1*, results in defects in sister chromatid cohesion (11,12), the process by which newly replicated chromatids remain physically associated until entry into anaphase. Moreover, *ctf18 rad24* double mutants have a mild S-M checkpoint defect that is not evident in either single mutant, and have a defect in Rad53 phosphorylation, a hallmark of the DNA damage response, indicating that Ctf18 also contributes to the S phase checkpoint response (13). Interestingly, *in vitro*, the Ctf18/Rfc2-5 complex can catalyze the loading and unloading of PCNA (14), however the biological significance of this activity is not well understood.

The Elg1–Rfc2-5 complex was recently identified as a member of the group of alternative RFCs in yeast and

*To whom correspondence should be addressed. Tel: +81 22 795 6875; Fax: +81 22 795 6873; Email: seki@mail.pharm.tohoku.ac.jp

human cells (2–4). Elg1/Rfc2-5 interacts with PCNA (4), but the PCNA-clamp loading activity of Elg1/Rfc2-5 has not been demonstrated. In the absence of *ELG1*, increased rates of spontaneous recombination were observed during vegetative growth in budding yeast (2). Allelic and ectopic intra and interchromosomal recombination, as well as recombination between sister chromatids, were elevated in this mutant (2). A high rate of chromosomal loss, transposition and mutation, and elevated levels of gross chromosomal rearrangements were also detected (2,3,15–17). In addition, mutations in *ELG1* resulted in elongation of telomeres, and increased silencing of subtelomeric genes (4,18). Mutants of *elg1* are sensitive to methylmethanesufonate (MMS) (3). In an *elg1 ctf18 rad24* triple mutant, MMS-induced Rad53 phosphorylation was completely abolished, whereas it was intact in the *elg1* single mutant (3,4). Thus, it seems likely that Elg1 is also involved in DNA repair; however this has yet to be confirmed.

One of the most dangerous DNA lesions is the DSB, which can be caused by ionizing radiation, or result from replication over single-strand breaks. When unrepaired, a DSB can cause permanent cell cycle arrest, and ultimately cell death. Several distinct mechanisms exist for the repair of DSBs (19,20). Accurate restoration of DNA broken ends can be achieved by HR, provided that homologous sequences are present elsewhere in the genome (21). In budding yeast, HR depends on the recombination factors Rad52–Rad51, which initiate the search for homologous sequences. Alternatively, a DSB can be repaired by direct ligation in a process termed nonhomologous end-joining (NHEJ). With some exceptions, NHEJ is mediated by the Ku heterodimer, which binds to double-stranded DNA ends and facilitates ligation (22).

In the current study, we demonstrated that the repair of DSBs induced by phleomycin is inefficient in *elg1* mutants. We also showed that in contrast to the high incidence of spontaneous recombination in *elg1* mutants, the absence of Elg1 did not result in an increase in the incidence of damage-induced recombination. Our results suggest that Elg1 functions in one or more of the steps of recombination repair itself. The implications of Elg1 function in homologous recombination (HR) will be discussed.

MATERIALS AND METHODS

Yeast strains

Yeast strains used in this study are listed in Supplementary Table S1. Null mutants, Myc-tagged, and HA-tagged alleles were made using standard PCR-based gene disruption and insertion methods, as described previously (23–25). To obtain the deletion mutants replaced by *KANMX6*, *HPHMX4* and *CgTRP1,* these genes were amplified from pFA6aKANMX6, pAG32 and SHB1805, respectively by using gene-specific primers consisting of 40–45 nt. The resulting PCR fragments were transformed into yeast cells and colonies that appeared on G418-, hygromycin B-containing YPAD plates or SC-Trp plates were isolated. Gene disruption was confirmed by genomic PCR. The Sequences of the primers used to generate the DNA constructs used for gene disruption, or for checking gene disruption, and details on the yeast strains used in study will be provided upon request.

Sensitivity to DNA damaging agents

For the analysis of sensitivity to continuous exposure to DNA damaging agents, 10-fold serial dilutions in distilled water of logarithmically growing cells (constructed as described above) were spotted onto YPAD plates, or YPAD plates containing the indicated concentrations of MMS, or phleomycin. The plates were incubated for 3 days at 30°C and then photographed. For NHEJ analysis, strains containing galactose-inducible HO endonuclease were grown overnight to 1×10^7 cells/ml in YP medium containing 2% raffinose. After washing once with water, aliquots of 10-fold serial dilutions were plated on YP medium containing 2% raffinose, supplemented with either 2% galactose or 2% glucose. The plates were incubated for 3 days at 30°C and then photographed. For the analysis of sensitivity to phleomycin, logarithmically growing cells were diluted to 10^7 cells/ml and cultured in the presence of 15 μg/ml nocodazole for 3 h to induce G_2/M phase arrest. G_2/M-arrested cells were exposed to 100 μg/ml phleomycin for 1 and 2 h. The cells were washed to remove phleomycin and nocodazole, diluted, and inoculated onto YPAD plates. After 3 days incubation at 30°C, colonies were counted.

Analysis of the incidence of interchromosomal HR between heteroalleles

Diploid strains with the MR101 background were constructed such that recombination between the heteroalleles *his1-1* and *his1-7* could be detected by the restoration of histidine prototrophy. As described previously (26), logarithmically growing cells were inoculated onto SC-His plates and YPAD plates containing various concentrations of MMS to evaluate the incidence of interchromosomal HR and colony forming cells (CFCs), respectively.

Pulsed-field gel electrophoresis (PFGE)

Logarithmically growing cells were diluted to 8×10^6 cells/ml and cultured in the presence of 15 μg/ml nocodazole for 3 h at 30°C to induce G_2/M phase arrest. G_2/M-arrested cells were exposed to 100 μg/ml phleomycin for 2 h at 30°C, washed to remove the phleomycin, and then cultured at 30°C in YPAD medium containing of 15 μg/ml nocodazole for the indicated periods of time. Agarose plugs containing chromosomal DNA were prepared as described previously, with minor modifications (27). All plugs were subsequently treated with Zymolyase 100T (0.15 mg/ml) and Proteinase K (1 mg/ml) at 30°C for 24 h. After electrophoresis, gels were stained with 0.5 μg/ml ethidium bromide for 30 min, destained in deionized water for 20 min, and then photographed.

Cell fractionation

Whole cell extracts (WCEs) and chromatin pellets were prepared as described previously (28), with the exception that spheroplasts were lysed in buffer containing Triton X-100 (EBX). WCEs were mixed with an equal volume of EBX buffer and incubated for 10 min. WCEs were then centrifuged through a sucrose cushion, and the resulting pellet was examined by immunoblot analysis for the presence of Elg1-13Myc. Histone H3 was used as a loading control for protein levels in WCEs and chromatin pellet (ChP) fractions.

Chromatin immunoprecipitation (ChIP)

ChIP was carried out as described previously, with minor modifications (29–32). Briefly, asynchronous cultures were grown overnight at 30°C in YP medium containing 2% raffinose. Nocodazole (15 μg/ml) was added to the cultures when they reached 6×10^6 cells/ml, and they were incubated at 30°C for 5 h to induce G_2/M phase arrest. Expression of HO endonuclease was then induced by adding 2% galactose. The cultures were washed 1 h after the addition of galactose, and then treated with 2% glucose to repress the expression of HO endonuclease. Cells were harvested, and incubated in 1% formaldehyde for 15 min to cross-link proteins to DNA, then the reaction was quenched by incubating cells in 125 mM glycine for 5 min. Cells were lysed with glass beads, and extracts were sonicated to shear DNA to an average size of 1 kb. Extracts were then divided into two aliquots: Input DNA and IP DNA (1:20, respectively). Immunoprecipitation was carried out using a monoclonal anti-Myc antibody (9E10) (Santa Cruz Biotechnology, Inc.), a monoclonal anti-HA antibody (12CA5) (Roche), or a polyclonal anti-PCNA antibody (kind gift from Dr Sugino), and immune complexes were captured using Dynabeads Protein G (Dynal Biotech) for 4 h at 4°C. After a series of washes, proteins were released from the beads by incubation for 6 h at 65°C. The samples were treated with protenase K, and DNA was purified for PCR analysis using phenol extraction, followed by ethanol precipitation.

PCR amplification

The following primers were used to amplify immunoprecipitated DNA: P1 (5′-TCCCCATCGTCTTGCTCT-3′) and P2 (5′-GCATGGGCAGTTTACCTTTAC-3′), which span the *MATZ* locus; P1 and P3 (5′-CCCAAGGCTTAGTATACACATCC-3′), which span the *HMLα* locus; or HO1-FW1 (5′-CCAGATTTGTATTAGACGAGGGACGGAGTGA-3′) and HO1-RV1 (5′-AGAGGGTCACAGCACTAATACAGCTCGTAAT-3′), which span the 2 kb region upstream of the HO endonuclease-induced DSB site. Primers SMC2-FW1 (5′-GACGACCTTGTAACAGTCCAGACAG-3′), and primer SMC2-RV1 (5′-GGCGAATTCCATCACATTATACTAACTACGG-3′), which anneal to the *SMC2* locus, were used as the controls. Amplified PCR products were separated by agarose gel electrophoresis, and quantitated using NIH image software. To correct for different levels of IP efficiency at different loci, the signal from the target locus was first normalized to the signal from an independent locus (*SMC2*) on chromosome VI, by dividing each target signal by the corresponding *SMC2* IP signal. For analysis of different time points, *MAT* or *HML* IP signals were normalized to the IP signal at 0 h, which was designated as 1. The data represents the average of three independent experiments. Error bars indicate the standard deviation.

In vivo physical monitoring of DSB induction, strand invasion and repair completion during recombination repair

DSB induction and strand invasion of input DNA were detected by PCR. The primers used for detection of DSB for *MAT*a strains (JKM161) or *MATα* (JKM179) strains were 5′-CTTTTAGTTTCAGCTTTCCG-3′ (pI)/5′-ACTCTATAAGGCCAAATGTACAAAC-3′ (pJ), and 5′-CTGGAAGTCAAAATACTCAGTTTCGACAG-3′ (pG)/5′-GGTGCATTTGTCATCCGTCCCGTATAGC-3′ (pH), respectively. The primers used to monitor primer extension and ligation were 5′-CTGGAAGTCAAAATACTCAGTTTCGACAG-3′ (pG)/5′-GGTGCATTTGTCATCCGTCCCGTATAGC-3′ (pH) and 5′-AGATGAGTTTAAATCCAGCATACTAG-3′ (pC)/5′-TGTTGTCTCACTATCTTGCCAATAAG-3′ (pD), respectively. The primer extension and ligation assays were carried out according to a previously described PCR-based method (33). Amplified PCR products were separated by agarose gel electrophoresis, and quantitated using NIH image software. The signal from the target locus was normalized to the amplified signal from an independent locus (*SMC2*) on chromosome VI. Primer extension and ligation were arbitrarily set at 100% for the highest wild-type level. The data represents the average of three independent experiments; error bars represent the SD.

RESULTS

Elg1 responds to phleomycin-induced DNA damage

Previously it was shown that *elg1* single deletion mutants are sensitive to MMS, but not to hydroxyl urea (HU) or ultraviolet (UV) light, and that Rad53 activation in response to MMS was similar in wild-type cells and *elg1* single mutants (3,4). These results suggested that Elg1 might also function in DNA repair. We extended this analysis by examining the sensitivity of the *elg1* single mutant to phleomycin as well as to MMS and HU. Phleomycin, like bleomycin, creates DNA DSBs, but in budding yeast, causes more significant DNA lesions than bleomycin (34,35). In addition to previously reported data that *elg1* mutants were sensitive to MMS (Figure 1A) (3), we further found that *elg1* mutants were also sensitive to phleomycin (Figure 1A). To further examine whether Elg1 binds to sites of DNA damage under conditions that preclude any potential interference of the DNA replication-related functions of Elg1, we analyzed the association of Elg1 with chromatin in G_2/M phase-arrested cells after the induction of DNA damage by MMS and pleomycin. As shown in Figure 1B, the amount of Elg1 in chromatin-containing fractions notably increased following exposure of cells to MMS or phleomycin, indicating that Elg1 functions in response to damaged DNA by binding to sites of DNA damage.

Elg1 is required for phleomycin-induced DSB repair in G_2/M phase-arrested cells

We investigate whether Elg1 is involved in DSB repair, because we notably found that *elg1* mutants are sensitive to phleomycin, which creates DSBs (34,35). On the other hands, deletion of *ELG1* causes defects in DNA replication (3,4), and the replication defects in *elg1* mutants could potentially cause sequestration of recombination machinery components (36). To avoid the potential influence of DNA replication-specific defects in *elg1* mutants, we examined the function of Elg1 in the repair of DSBs induced by phleomycin in G_2/M phase-arrested cells. As seen in Figure 2A,

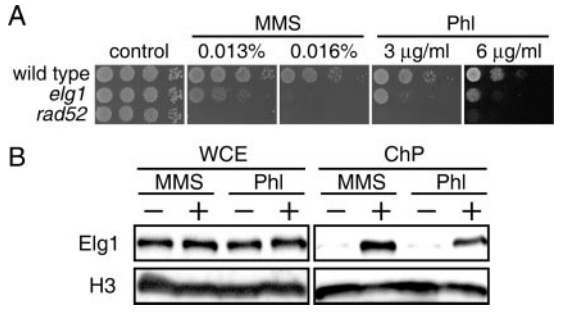

Figure 1. Elg1 is involved in the response to phleomycin-induced DNA damage. (**A**) Viability of wild-type (SCRL), *elg1* (YHO601) and *rad52* (YHO602) mutants in the presence of MMS and phleomycin (Phl). (**B**) G_2/M-arrested cells expressing Elg1-13Myc (YHO501) were exposed to 0.2% MMS or 100 μg/ml phleomycin for 2 h. Cell aliquots were taken before exposure (−), and 2 h after MMS or phleomycin (Phl) exposure (+). Whole cell extract (WCE) and chromatin pellets (ChP) were prepared, and analyzed by immunoblot for the presence of the indicated proteins. Histone H3 was used as a loading control for protein levels in WCE and ChP fractions. Elg1-13myc and Histone H3 were detected using anti-Myc monoclonal antibody, and anti-Histone H3-specific antibody, respectively.

elg1 cells arrested in G_2/M phase showed a higher sensitivity to phleomycin than wild-type cells; however this result does not necessarily exclude the possibility that *elg1* cells are sensitive to phleomycin in other phases of the cell cycle. To monitor the formation and subsequent repair of DSBs, cells arrested in G_2/M were treated with phleomycin, and then cultured in phleomycin-free medium containing nocodazole to maintain G_2/M arrest (Figure 2B). Chromosomal DNA was isolated and subjected to PFGE. Distinct chromosomal bands were absent following exposure to phleomycin in both wild-type and *elg1* cells, and concurrently, a low-molecular-weight DNA smear appeared, reflecting the accumulation of DNA DSBs (Figure 2C). Restoration of chromosome-sized DNA bands was observed in both wild-type and *elg1* mutants after culture in phleomycin-free medium. However, the reappearance of distinct chromosomal bands was less efficient in *elg1* mutants compared to wild-type cells. These results suggested that Elg1 is involved in DSB repair.

Elg1 is required for HR repair

DSBs can be repaired by the NHEJ pathway, which requires Yku70, or the HR pathway, which requires Rad52 (37–39). We next examined whether Elg1 was required for NHEJ-mediated or HR-mediated repair. To examine the involvement of Elg1 in NHEJ, single chromosomal DSB was induced in the *MAT* locus by expressing HO endonuclease in a galactose-dependent manner, in an *elg1* mutant strain in which use of the HR-mediated repair pathway was precluded, due to deletion of the homologous donor loci, *HML* and *HMR* (Figure 3A). Sustained expression of HO endonuclease leads to a continuous cycle of DNA cleavage and ligation. If cells are competent for error-prone repair by NHEJ, they will be able to grow in the presence of HO endonuclease, while cells deficient in NHEJ will not survive (40,41). When we examined the viability of *elg1* and *rad52* mutants under sustained expression of HO endonuclease, we failed to detect a decrease in survival compared to

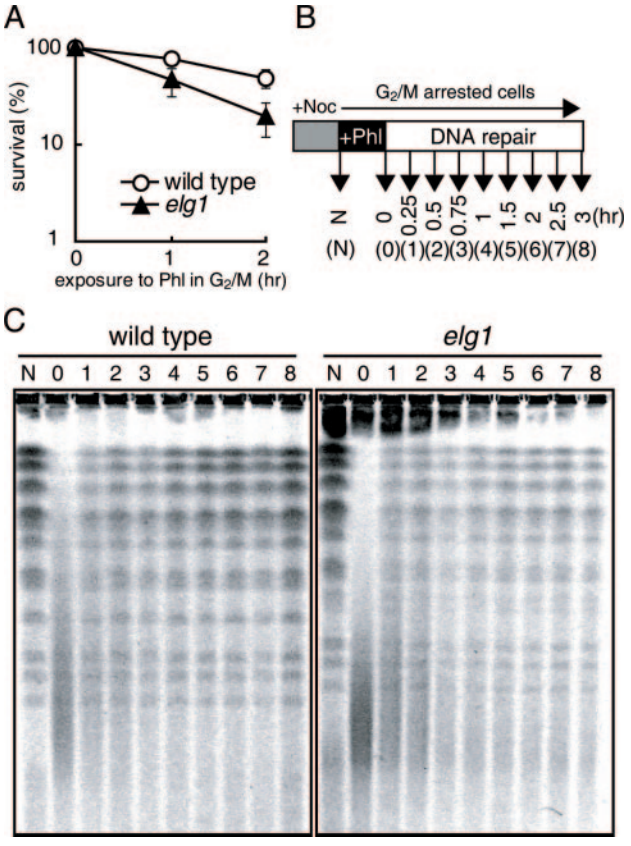

Figure 2. Involvement of Elg1 in the repair of phleomycin-induced DNA damage in G_2/M phase. (**A**) Sensitivity to phleomycin of cells arrested in G_2/M. Cells (wild-type; MR101, *elg1*; YHO215) arrested in the G_2/M phase were exposed to phleomycin (100 μg/ml) at 30°C for the indicated periods of time, washed to remove phleomycin, inoculated onto YPAD plates containing neither phleomycin nor nocodazole, and incubated for 3 days at 30°C before counting colonies. To measure the sensitivity to phleomycin, at least four cultures were taken for each point. The data represents the means and standard error. (**B**) Schematic representation of the process used to prepare the cells in PFGE. (**C**) Representative gel image. G_2/M-arrested cells (wild-type; MR101, *elg1*; YHO215) were exposed to 100 μg/ml phleomycin at 30°C for 2 h, and then cultured in phleomycin-free medium containing nocodazole for the indicated periods of time. The cells were harvested, and their DNA was analyzed by PFGE as described in Materials and Methods. Lane N: untreated cells; Lane 0: cells treated with phleomycin for 2 h; Lanes 1, 2, 3, 4, 5, 6, 7, 8: cells treated with phleomycin for 2 h, then cultured in phleomycin-free medium for 0.25, 0.5, 0.75, 1.0, 1.5, 2.0, 2.5, 3.0 h, respectively.

wild-type cells. In contrast, the viability of *yku70* mutants was decreased (Figure 3B). These results indicated that Elg1 is not important for DSB repair by NHEJ.

To examine the involvement of Elg1 in HR, we investigated for an interchromosomal recombination event between heteroalleles *his1-1*/*his1-7*, using diploid *elg1* single mutant cells (Figure 3C). We observed an increase in spontaneous recombination in *elg1* mutants compared to wild-type cells (Figure 3D), as reported previously (2). The incidence of heteroallelic recombination in wild-type cells increased with increasing concentrations of MMS (Figure 3E). In comparison, the recombination frequency in *elg1* mutants was lower than that of wild-type cells. Moreover, the recombination frequency following exposure to phleomycin was also lower in *elg1* mutants compared to wild-type cells

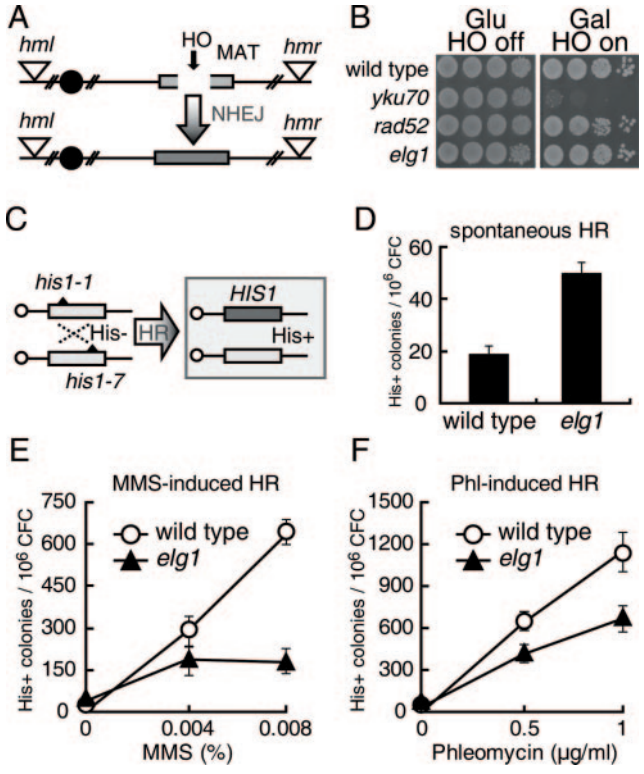

Figure 3. Elg1 is involved in damage-induced recombination repair. (**A**) Schematic representation of the process and outcome of NHEJ at the galactose-inducible HO endonuclease specific DSB site on chromosome III in yeast strain JKM179. (**B**) The NHEJ DSB repair pathway is intact in *elg1* mutants. Viability of wild-type (JKM179), *yku70* (YHO505), *rad52* (YHO506) and *elg1* (YHO504) mutants in the background of an HR repair defective yeast strain grown on either glucose (HO off), or galactose (HO on). A galactose-inducible HO endonuclease was integrated at the *ADE3* locus of a haploid yeast strain that was defective in HR-mediated DSB repair. Upon switching the cells to galactose, HO endonuclease is expressed, inducing a single DSB at the *MAT* locus. Functional DSB repair can occur only through the NHEJ pathway in this strain, since the *HM* donor loci, *HML* and *HMR*, are deleted. (**C**) Schematic representation of the process and outcome of heteroallele recombination at the *HIS1* locus. (**D–F**) Heteroallelic recombination at the *HIS1* locus. Frequency of spontaneous recombination (D), MMS-induced recombination (E) and phleomycin-induced recombination (F) in wild-type and e*lg1* mutant cells. Wild-type (MR101) and *elg1* (YHO215) mutant cells were inoculated onto YPAD plates, or SC plates lacking His and containing the indicated concentrations of MMS or phleomycin, then incubated at 30°C for 3 days. The frequency of HR is presented as the number of His^+ colonies per 10^6 CFC. To measure recombination frequency, at least four cultures were taken for each point. The data represents the means and standard deviation.

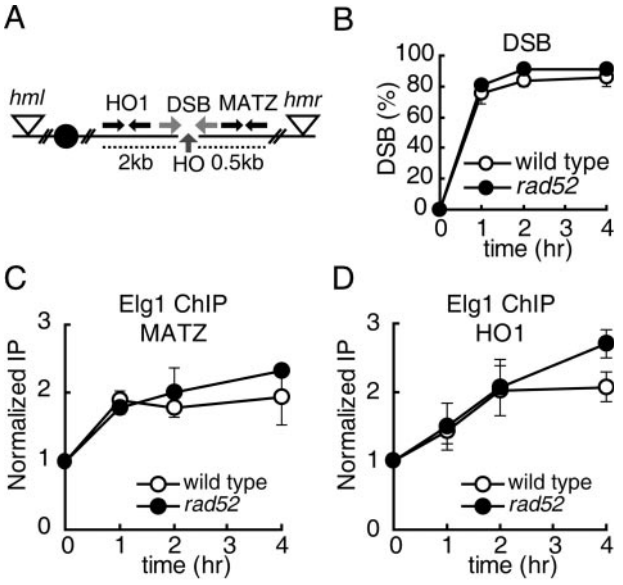

Figure 4. Elg1 is recruited to DSB sites *in vivo* in G_2/M phase. (**A**) Schematic representation of the galactose-inducible HO endonuclease specific DSB site on chromosome III in yeast strain JKM179. The two arrows on either side of the DSB show the location of the primers used to detect induction/efficiency of DSBs by HO endonuclease (DSB primers). Also depicted are the *HO1* and *MATZ* loci flanking the DSB site, and the locations of the PCR primers used to amplify these segments of DNA (HO1 and MATZ primers, respectively). (**B**) Kinetics of DSB induction. Wild-type (YHO501), *rad52* (YHO502) cells expressing Elg1-13myc were arrested in G_2/M phase in 2% raffinose at 30°C, then shifted to 2% galactose to induce expression of HO endonuclease and DSBs. Genomic DNA was harvested at the indicated time points after the shift. PCR was carried using 'input DNA' (see Materials and Methods), and DSB primers, which flank the HO cleavage site. Amplification of the *SMC2* locus on chromosome VI was used as a control. Cleavage efficiency (% DSBs) at each time point was calculated as the ratio of *MATa: SMC2* signal, normalized to that of un-induced cells (zero time point). (**C** and **D**) Cells were treated as described in B, and genomic DNA from cells at the indicated time points after HO endonuclease induction was subjected to ChIP analysis using anti-Myc antibodies. Levels of CEN-distal (MATZ) (C) or CEN-proximal (HO1) (D) DNA in anti-Myc immune complexes were quantified, and normalized to the *SMC2* control fragment. Each time point was then normalized to the zero time point value. Data represents the means and SD of three independent experiments. Representative photographs of agarose gels in (C and D) are shown in Supplementary Figure S1.

(Figure 3F). These results suggested that Elg1 is required for efficient execution of damage-induced HR.

Elg1 association around DSB sites did not depend on Rad52

To characterize the sites of association of Elg1 in detail, we examined Elg1 recruitment to a single chromosomal DSB site in G_2/M phase-arrested cells. Initially, we examined the kinetics of Elg1 recruitment to DNA sequences on both sides of the DSB site using yeast strain JKM179, which lacks both the *HML* and *HMR* homologous donor sequences, in order to more easily capture the initial binding of proteins to the DSB site (Figure 4A). A DSB in the *MAT* locus was induced by expression of HO endonuclease in JKM179 yeast expressing Myc-tagged Elg1 (Elg1-13Myc), and at various time points after induction (0, 1, 2 and 4 h), cell aliquots were removed and treated with formaldehyde to induce crosslinking of proteins to DNA, then subjected to ChIP analysis. Immunoprecipitated DNA was analyzed by PCR for the presence of *MAT*-specific sequences from both sides of the DSB (CEN-proximal site, HO1; CEN-distal site, MATZ) (Figure 4A). PCR primers corresponding to sequences in the *SMC2* locus (an independent locus on chromosome VI) were used as a control. Since the immunoprecipitation efficiency at each amplicon was different, amplified products were normalized to the zero time point value (Normalized IP). As seen in Figure 4B, following induction of HO endonuclease expression, the DSB at the *MAT* locus was induced rapidly and efficiently. Remarkably, binding of Elg1 to DNA sequences on both sides of the DSB break site increased 2-fold after induction of HO endonuclease expression and DSBs (Figure 4C and D). We also examined whether the

binding of Elg1 around the DSB site was dependent on Rad52, which plays a major role during HR. The induction of DSB occurred in a similar manner in *rad52* mutants and wild-type cells (Figure 4C and D). Importantly, we found that the association of Elg1 with the MATZ and HO1 sites was not dependent on Rad52 (Figure 4C and D).

Elg1 is recruited to homologous donor sites depending on Rad52

HR-mediated chromosomal DSB repair is a multiple-step process that includes recruitment of DNA repair enzymes to the DSB site, strand invasion by a homologous template, DNA synthesis, resolution of Holliday junctions and ligation. One of the best characterized systems for studying HR is HO endonuclease-induced *MAT* switching, using *HML* as the donor template (42). In this system, repair of the HO endonuclease-induced DSB in the *MAT*a locus is accomplished through recombination with the homologous *HML*α locus. We investigated DSB repair by HR in wild-type and *rad52* mutants, using strain JKM161, which contains *HML*α *MAT*a as the donor template. By using a galactose-inducible *GAL::HO* gene, we were able to induce a DSB synchronously in all cells of the population. DSB formation at the HO recognition site and invasion of the *MAT* recipient strand into the donor strand (*HML*) were monitored by PCR using the primers shown in Figure 5A. The amount of PCR product corresponding to the *MAT*a locus was considerably decreased 1 h after induction of HO endonuclease in wild-type cells and *rad52* mutants; that is, cleavage at the *MAT* locus occurred within 1 h with high-efficiency. Strand invasion was detected 2 and 4 h after induction of HO in wild-type cells but not in *rad52* mutants, as expected (Figure 5B).

To examine whether Elg1 was recruited to both the *MAT* recipient locus and the *HML* donor locus during the process of recombination, we performed ChIP analysis using the primers shown in Figure 5C. Under the conditions in Figure 4B, the association of Elg1 with the DSB site in the *MAT* locus was observed 1 h after induction of HO endonuclease in wild-type cells and *rad52* mutants (Figure 5D). Importantly, the association of Elg1 with the *HML* donor strand was also observed and increased during incubation (Figure 5E). However, the association of Elg1 with the *HML* donor strand was not observed in *rad52* mutants (Figure 5E), suggesting that Elg1 is recruited to DNA region required for HR repair.

Late stages of HR repair are inefficiently completed in *elg1* mutants

We next examined whether Elg1 was necessary for extension of the invading *MAT* DNA strand of the homologous *HML*α donor site, a step which requires DNA polymerization. DSB formation at the HO recognition site, primer extension following strand invasion on the donor strand and completion of repair (ligation) were monitored by PCR, using the primers shown in Figure 6A. Formation of a DSB occurred with the same kinetics in *elg1* mutants and wild-type cells (Figure 6B). In contrast, extension of the invading DNA strand was slightly reduced in *elg1* mutants, compared to wild-type cells (Figure 6C; left panel). Following strand invasion and resolution of Holliday junctions, the process

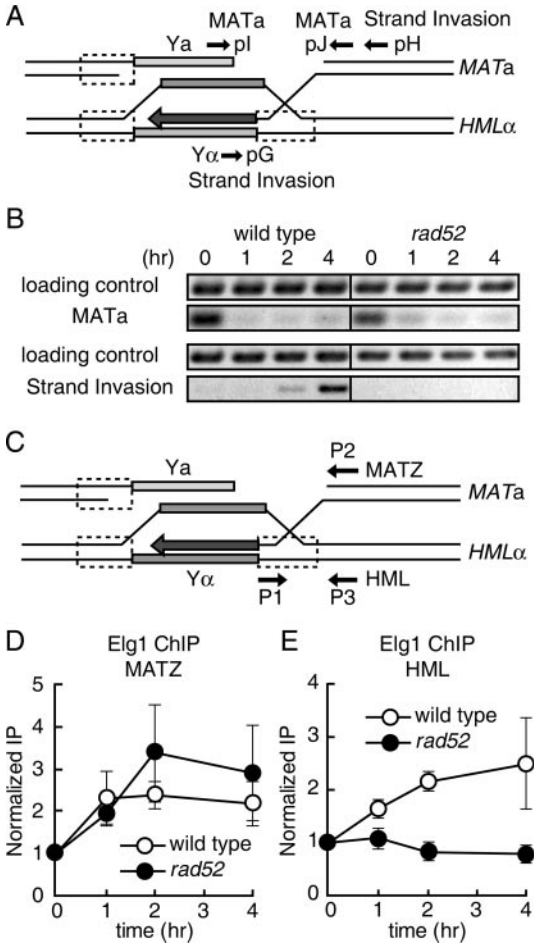

Figure 5. Elg1 is recruited onto homologous donor sites during recombination repair in G_2/M phase. DSBs were induced in G_2/M-arrested JKM161cells expressing Elg1-3HA and carrying the *HML* donor sequence by treating cells with 2% galactose for 1 h to induce expression of HO endonuclease, followed by incubation in 2% glucose to repress HO endonuclease expression. Genomic DNA was isolated at the indicated time points after the addition of galactose. (**A**) Schematic representation of the HR intermediates formed during mating-type switching. The approximate location of the primers used to monitor DSBs (pI and pJ primers), and strand invasion (pG and pH primers) are indicated. (**B**) Time course of DSB formation and formation of strand invasion intermediates following induction of HO endonuclease expression. DNA was purified from cells at the indicated time points after transient expression of HO endonuclease. PCR was carried out using primers that flanked the *MATa* locus (pI and pJ primers) to detect formation of the DSB (upper panel), or pG and pH primers to detect products of strand invasion and primer extension (lower panel). The *SMC2* locus was amplified as a loading control. The data in the chart is representative of three independent experiments. (**C**) Schematic representation of the *MAT* and *HML* loci, showing the location of the primers used to detect association of Elg1 with sequences at the DSB site (P1 and P2 primers for the CEN-distal *MATZ* locus) or the homologous donor region (P1 and P3 primers for the *HML locus*) (**D** and **E**) wild-type (YHO406) and *rad52* mutant (YHO407) cells expressing Elg1-3HA were treated as described for (B), and chromatin from cells at the indicated time points after addition of galactose was subjected to immunoprecipitation using anti-HA antibodies. DNA present in anti-HA immune complexes was analyzed by PCR using primers specific for sequences at the DSB site (P1 and P2 primers for the CEN-distal *MATZ* locus) or the homologous donor region (P1 and P3 primers for the *HML* locus), as indicated. Data from each target locus was normalized to the control *SMC2* product. Fold-increase was calculated by normalizing the data from each time point to the zero time point value. Data represents the averages and standard deviation of three independent experiments. Quantified data obtained from quantitative real-time PCR are shown in Supplementary Figure S2.

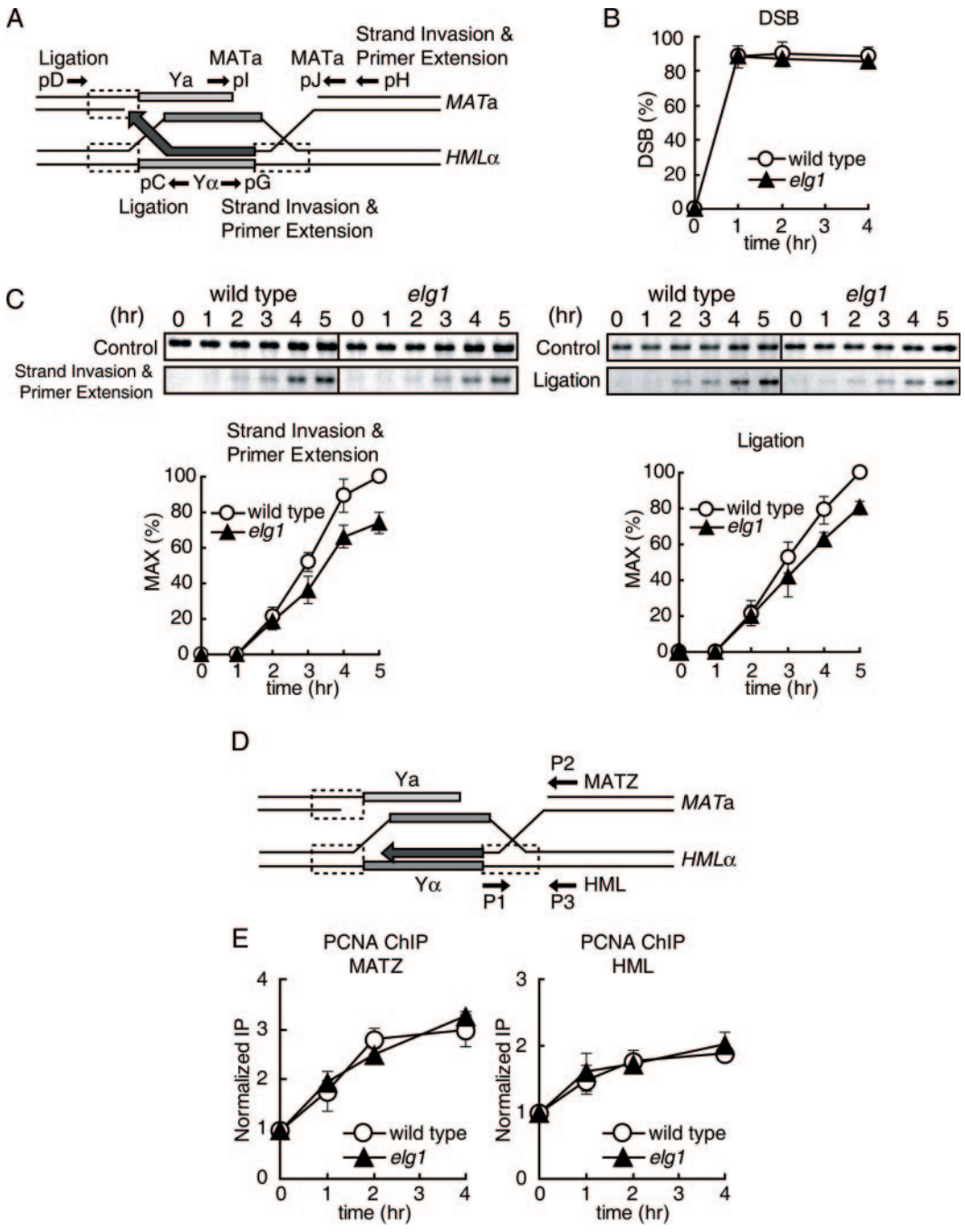

Figure 6. *elg1* mutants are defective in late steps of recombination repair in G_2/M phase. G_2/M-arrested JKM161 cells carrying the *HML* donor sequence were treated as described for Figure 5. (**A**) Schematic representation of the HR intermediates formed during mating-type switching. The approximate location of the primers used to monitor DSBs (pI and pJ; MATa primers), strand invasion and primer extension (pG and pH; strand invasion and primer extension primers), and completion of repair (pC and pD; ligation primers) are indicated. (**B**–**D**) Genomic DNA was isolated from wild-type (JKM161), and *elg1* mutant (YHO408) cells at the indicated time points after transient expression of HO endonuclease, and subjected to PCR analysis to determine the efficiency of DSB formation (B), strand invasion and primer extension [(C); left panels], and completion of repair (ligation) [(C); right panels]. Amplified PCR products were run on agarose gels and stained with ethidium bromide. Representative gel images of strand invasion, primer extension and completion of repair (ligation) are shown [(C); upper panels]. DNA signals were quantified and then normalized to the control *SMC2* product. A PCR product using primers specific for detecting the strand invasion and primer extension step will only be generated if 3′ strand invasion and replication of at least 222 nt of the donor template sequence occurs. The highest level of strand invasion-primer extension and completion of repair (ligation), in wild-type cells was designated as 100%. The data represents the averages and SD of three independent experiments. (D) Schematic representation of the *MAT* and *HML* loci, showing the location of the primers used to detect association of PCNA with sequences at the DSB site (P1 and P2 primers for the *CEN*-distal *MAT* locus) or the homologous donor region (P1 and P3 primers for the *HML locus*). (**E**) Wild-type (JKM161) and *elg1* mutant (YHO408) cells arrested in G_2/M phase were treated as described for Figure 5, and chromatin from cells at the indicated time points after addition of galactose was subjected to immunoprecipitation using anti-PCNA antibodies. DNA present in anti-PCNA immune complexes was analyzed by PCR using primers specific for sequences at the DSB site (P1 and P2 primers for the *CEN*-distal *MAT* locus; left panel) or the homologous donor region (P1 and P3 primers for the *HML* locus; right panel), as indicated. Data from each target locus was normalized to the control *SMC2* product. Fold-increase was calculated by normalizing the data from each time point to the zero time point value. Data represents the averages and SD of three independent experiments.

of recombination repair is completed by DNA ligation. We monitored the completion of repair following extension of the invading DNA strand in *elg1* mutants. In *elg1* mutants, the completion of the late stage, post-synaptic DNA repair step was slightly delayed and reduced compared to wild-type cells (Figure 6C; right panel).

Effect of Elg1 on the recruitment of PCNA to the *MAT* recipient locus and the homologous *HMLα* donor site

Elg1 and PCNA physically interact with each other (4). Moreover, over-expression of PCNA rescued the MMS sensitivity of *elg1* mutants (3). Mutation of PCNA (*POL30*) results in a defect in primer extension during HO-induced HR (43), suggesting that Elg1 is required for loading of PCNA during recombination repair. We observed that the amount of PCNA, as well as Elg1, in chromatin-containing fractions notably increased following exposure to MMS or phleomycin (data not shown). To examine whether PCNA was recruited to the *MAT* recipient and the *HML* donor loci during the process of recombination, we performed ChIP analysis using the primers shown in Figure 6D. The association of PCNA with the *MAT* recipient and the *HML* donor loci was observed in both *elg1* mutants and wild-type cells (Figure 6E). Unexpectedly, the level of association of PCNA with these loci was almost the same in *elg1* mutants and wild-type cells.

DISCUSSION

In the current study, we examined the role of Elg1 in the DNA damage response in *S.cerevisiae*. Previous reports have suggested that Elg1 might function as a checkpoint sensor, similar to the RFC-like checkpoint protein Rad24, because *elg1 rad24 ctf18* triple mutants, which do not contain alternative RFC-like proteins, are completely defective in intra-S checkpoint control (3,4). Although the *elg1* single mutant is sensitive to DNA damaging agents, it is reportedly not defective in the activation of the DNA damage checkpoint (3).

The main finding of this study is that the Rfc1-like protein Elg1 participates in DNA damage-induced recombination repair itself. It was previously shown that deletion of *ELG1* increases the incidence of spontaneous recombination in yeast (2). Previous studies have shown that an elevated frequency of mitotic recombination is a signal of DNA replication defects (44,45), and it has been proposed that Elg1 is involved in efficient lagging strand DNA synthesis (3,4). Accordingly, one of the potential explanations for the observed spontaneous hyper-recombination of *elg1* mutants is that these cells are defective in DNA replication. In contrast to spontaneous recombination, we found that the frequency of MMS- or phleomycin-induced recombination was decreased in *elg1* mutants compared to wild-type cells (Figure 3).

To avoid potential complications due to defects in DNA replication in *elg1* mutants, we examined the function of Elg1 in G_2/M phase-arrested cells. We showed that the repair efficiency of phleomycin-induced DSB in *elg1* mutants was lower than wild-type cells in G_2/M phase (Figure 2). In the HO endonuclease-induced recombination system, Elg1 associated with both sides of the HO-induced DSB site (Figure 4), suggesting that Elg1 plays a role in early events in HR or the damage response. In response to DSBs, the MRX complex, a heterotrimeric protein assembly of Mre11, Rad50 and Xrs2, arrives first at DSB sites and performs nucleolytic resection to generate single-stranded DNA (ssDNA). This is essential for subsequent protein assembly (46). ssDNA is recognized by the ssDNA binding protein RPA, and the DNA damage checkpoint factors, Rad24-RFC and Ddc1/Mec3/Rad17, are recruited in RPA-dependent manner. Lastly, the proteins that are directly involved in HR are recruited to the DSB site. The assembly of HR proteins on ssDNA is initiated by Rad52, which in turn causes strand invasion. We found that the association of Elg1 with DSB sites was not dependent on Rad52 (Figure 4). Importantly, we found that Elg1 is also recruited to the *HML* donor locus, and that this was dependent on the function of Rad52 (Figure 5E), suggesting that Elg1 functions in HR after strand invasion has occurred. Alternatively, it may not be the donor locus *per se* that is associated with Elg1. In other words, the donor locus may only engage in preferential interaction with Elg1 when it has already formed a Holliday junction with the invading end. Thus, the interaction between Elg1 and the donor locus is probably a consequence of the complex that originally formed at the double-stranded break.

The *MAT* switching system provides a good model for DSB repair based on synthesis dependent strand annealing (SDSA) (36,47). In this system, DNA synthesis is initiated from the end of the invading strand, as in leading-strand synthesis. The newly synthesized DNA is displaced from the template (*MATY*α region), returned to the original strand, and ligated (Figure 6A). After the removal of the non-homologous region (*MATY***a**) at the DSB site by probably Rad1-Rad10 and Msh2-Msh3 (48,49), DNA synthesis is initiated from the second end of the DSB using the returning strand as the template, as in leading-strand synthesis, followed by ligation to form an intact double-strand. Of note, mutation of either RFC (*CDC44*) or PCNA (*POL30*) results in a defect in primer extension during HO-induced HR (43), suggesting that the RFC1 complex is required for loading of PCNA during DNA repair as well. It has been shown that Elg1 and PCNA physically interact with each other (4). Moreover, over-expression of PCNA rescued the MMS sensitivity of *elg1* mutants (3). In the current study, we show that *elg1* mutants are partially defective in MMS-induced recombination (Figure 3E), and Elg1 is also recruited to the homologous donor locus depending on Rad52 (Figure 5E). Recombination assay showed 2- to 4-fold reduction of MMS- or phleomycin-induced recombination frequency in *elg1* mutants compared to wild-type cells (Figure 3E and F). In addition, we carried out PCR-based analysis of the efficiency of primer extension from the invaded strand, and ligation of the synthesized strand after induction of HO-induced DSB. The efficiency of primer extension and ligation of the synthesized strand slightly decreases in *elg1* mutants (Figure 6C). It seems likely that the defect in *elg1* mutants lies at the primer extension step or a step earlier than primer extension. Although it is unknown how Elg1 is recruited onto the donor sites at the molecular level, the interaction of Elg1 with the donor sites seems to facilitate the above steps in HR via PCNA-mediated DNA synthesis. Then we investigated the association of PCNA with the *HML* locus as well as the

MATZ locus after induction of DSB by HO endonuclease, and confirmed the association of PCNA with these loci. Unexpectedly, the amount of PCNA associated these loci did not differ between *elg1* mutants and wild-type cells (Figure 6E), suggesting that Elg1 might be not involved in the loading of PCNA during HR. The defect in HO-induced HR repair in *elg1* mutants was relatively mild compared to that observed in phleomycin-induced HR. This may reflect the fact that the total number of DSBs induced by phleomycin is quite large, compared to the single DSB induced by HO endonuclease expression. Thus, we could not exclude the possibility that the sensitivity of ChIP assay was too low to detect the small difference between *elg1* mutants and wild-type cells due to main requirement of canonical RFC for the loading of PCNA.

If Elg1 is not involved in the loading of PCNA, what is the function of Elg1 in HR? It has been reported that mutants of DNA polymerase δ (Pol3) and ε (Pol2), *pol3-14* and *pol2-18*, show a mild defect in HR repair, while the PCNA mutants (*pol30-52*) are completely defective in HR (36). Taken together, it seems conceivable that Elg1 plays a role in the efficient recruitment of either DNA polymerase δ or ε, directly or indirectly, by interacting with PCNA, or in choosing or switching to the optimum DNA polymerase for repair synthesis.

It has been reported that *sgs1* cells, which show spontaneous hyper-recombination, are defective in damage-induced recombination (50,51). Thus, it is not surprising that *elg1* cells show not only spontaneous hyper-recombination but an apparent damage-induced hypo-recombination. Spontaneous hyper-recombination is one of the hallmarks of a defect in DNA replication, because many temperature sensitive mutants in DNA replication show hyper-recombination phenotypes. In agreement with the above notion, *elg1* cells show some defects in DNA replication (3,4). The classical RFC complex (without Elg1) is probably adequate for the mediation of the protein interactions required for the DNA repair process during normal growth (low level of DNA damage). However, upon induction of massive DNA damage, the classical RFC complex probably cannot accommodate any longer the full cellular demand for DNA repair. Thus, Elg1 is more important under damage-induced conditions than during normal cell growth. Even small defects in genome maintenance mechanisms should not be dismissed, however, as they may exert a significant influence on the fitness of an organism. Thus, *ELG1* is an attractive candidate as a novel anti-oncogene, as its deletion seems to result in significant genome instability, which is associated with an increased risk for cancer (52).

SUPPLEMENTARY DATA

Supplementary Data are available at NAR online.

ACKNOWLEDGEMENTS

The authors thank Drs A. Sugino Y. Kawasaki, M. Arisawa, and J. E. Haber for plasmids, antibody or strains used in the study. The authors thank all members of the Enomoto lab for their support. This work was supported by Grants-in-Aid for Scientific Research on Priority Areas from The Ministry of Education, Science, Sports and Culture of Japan. Funding to pay the Open Access publication charges for this article was provided by Grant-in-Aid for Scientific Research on Priority Areas from The Ministry of Education, Science, Sports and Culture of Japan.

Conflict of interest statement. None declared.

REFERENCES

1. Kolodner,R.D., Putnam,C.D. and Myun,K. (2002) Maintenance of genome stability in *Saccharomyces cerevisiae*. *Science*, **297**, 552–557.
2. Ben-Aroya,S., Koren,A., Liefshitz,B., Steinlauf,R. and Kupiec,M. (2003) ELG1, a yeast gene required for genome stability, forms a complex related to replication factor C. *Proc. Natl Acad. Sci. USA*, **100**, 9906–9911.
3. Bellaoui,M., Chang,M., Ou,J., Xu,H., Boone,C. and Brown,G.W. (2003) Elg1 forms an alternative RFC complex important for DNA replication and genome integrity. *EMBO J.*, **22**, 4304–4313.
4. Kanellis,P., Agyei,R. and Durocher,D. (2003) Elg1 forms an alternative PCNA-interacting RFC complex required to maintain genome stability. *Curr Biol.*, **13**, 1583–1595.
5. Tsurimoto,T. and Stillman,B. (1989) Purification of a cellular replication factor, RF-C, that is required for coordinated synthesis of leading and lagging strands during simian virus 40 DNA replication in vitro. *Mol. Cell. Biol.*, **9**, 609–619.
6. Virshup,D.M. and Kelly,T.J. (1989) Purification of replication protein C, a cellular protein involved in the initial stages of simian virus 40 DNA replication *in vitro*. *Proc. Natl Acad. Sci. USA*, **86**, 3584–3588.
7. Hubscher,U., Maga,G. and Podust,V. (1996) DNA replication accessory proteins. In De Pamphilis,M. (ed.), *DNA Replication in Eukaryotic Cells*. Cold Spring Harbor Laboratory Press, Cold Spring Harbor, NY, pp. 525–543.
8. Mossi,R. and Hubscher,U. (1998) Clamping down on clamps and clamp loaders-the eukaryotic replication factor C. *Eur. J. Biochem.*, **254**, 209–216.
9. Green,C.M., Erdjument-Bromage,H., Tempst,P. and Lowndes,N.F. (2000) A novel Rad24 checkpoint protein complex closely related to replication factor C. *Curr. Biol.*, **10**, 39–42.
10. Majka,J. and Burgers,P.M. (2003) Yeast Rad17/Mec3/Ddc1: a sliding clamp for the DNA damage checkpoint. *Proc. Natl Acad. Sci. USA*, **100**, 2249–2254.
11. Hanna,J.S., Kroll,E.S., Lundblad,V. and Spencer,F.A. (2001) *Saccharomyces cerevisiae* CTF18 and CTF4 are required for sister chromatid cohesion. *Mol. Cell. Biol.*, **21**, 3144–3158.
12. Mayer,M.L., Gygi,S.P., Aebersold,R. and Hieter,P. (2001) Identification of RFC (Ctf18p, Ctf8p, Dcc1p): an alternative RFC complex required for sister chromatid cohesion in *S.cerevisiae*. *Mol. Cell*, **7**, 959–970.
13. Naiki,T., Shimomura,T., Kondo,T., Matsumoto,K. and Sugimoto,K. (2000) Rfc5, in cooperation with rad24, controls DNA damage checkpoints throughout the cell cycle in *Saccharomyces cerevisiae*. *Mol. Cell. Biol.*, **20**, 5888–5896.
14. Bylund,G.O. and Burgers,P.M. (2005) Replication protein A-directed unloading of PCNA by the Ctf18 cohesion establishment complex. *Mol. Cell. Biol.*, **13**, 5445–5455.
15. Scholes,D.T., Banerjee,M., Bowen,B. and Curcio,M.J. (2001) Multiple regulators of Ty1 transposition in *Saccharomyces cerevisiae* have conserved roles in genome maintenance. *Genetics*, **159**, 1449–1465.
16. Huang,M.E., Rio,A.G., Nicolas,A. and Kolodner,R.D. (2003) A genomewide screen in *Saccharomyces cerevisiae* for genes that suppress the accumulation of mutations. *Proc. Natl Acad. Sci. USA*, **100**, 11529–11534.
17. Smith,S., Hwang,J.Y., Banerjee,S., Majeed,A., Gupta,A. and Myung,K. (2004) Mutator genes for suppression of gross chromosomal rearrangements identified by a genome-wide screening in *Saccharomyces cerevisiae*. *Proc. Natl Acad. Sci. USA*, **101**, 9039–9044.
18. Smolikov,S., Mazor,Y. and Krauskopf,A. (2004) A ELG1, a regulator of genome stability, has a role in telomere length regulation and in silencing. *Proc. Natl Acad. Sci. USA*, **101**, 1656–1661.

19. Aylon,Y. and Kupiec,M. (2004) DSB repair: the yeast paradigm. *DNA Repair*, **3**, 797–815.
20. Haber,J.E. (2000) Partners and pathways: repairing a double-strand break. *Trends Genet*., **16**, 259–264.
21. Haber,J.E. (1999) DNA recombination: the replication connection. *Trends Biochem. Sci*., **24**, 271–275.
22. Downs,J.A. and Jackson,S.P. (2004) A means to a DNA end: the many roles of Ku. *Nature Rev. Mol. Cell. Biol*., **5**, 367–378.
23. Goldstein,A.L. and McCusker,J.H. (1999) Three new dominant drug resistance cassettes for gene disruption in *Saccharomyces cerevisiae*. *Yeast*, **15**, 1541–1553.
24. Kitada,K., Yamaguchi,E. and Arisawa,M. (1995) Cloning of the *Candida glabrata* TRP1 and HIS3 genes, and construction of their disruptant strains by sequential integrative transformation. *Gene*, **165**, 203–206.
25. Wach,A. (1996) PCR-synthesis of marker cassettes with long flanking homology regions for gene disruptions in *S. cerevisiae*. *Yeast*, **12**, 259–265.
26. Ui,A., Satoh,Y., Onoda,F., Miyajima,A., Seki,M. and Enomoto,T. (2001) The N-terminal region of Sgs1, which interacts with Top3, is required for complementation of MMS sensitivity and suppression of hyper-recombination in sgs1 disruptants. *Mol. Genet. Genomics*, **265**, 837–850.
27. Ui,A., Seki,M., Ogiwara,H., Onodera,R., Fukushige,S., Onoda,F. and Enomoto,T. (2005) The ability of Sgs1 to interact with DNA topoisomerase III is essential for damage-induced recombination. *DNA Repair*, **4**, 191–201.
28. Liang,C. and Stillman,B. (1997) Persistent initiation of DNA replication and chromatin-bound MCM proteins during the cell cycle in cdc6 mutants. *Genes Dev*., **11**, 3375–3386.
29. Huang,J. and Moazed,D. (2003) Association of the RENT complex with nontranscribed and coding regions of rDNA and a regional requirement for the replication fork block protein Fob1 in rDNA silencing. *Genes Dev*., **17**, 2162–2176.
30. Sugawara,N., Wang,X. and Haber,J.E. (2003) *In vivo* roles of Rad52, Rad54 and Rad55 proteins in Rad51-mediated recombination. *Mol. Cell*, **12**, 209–219.
31. Wolner,B., Van Komen,S., Sung,P. and Peterson,C. (2003) Recruitment of the recombinational repair machinery to a DNA double strand break in yeast. *Mol. Cell*, **12**, 221–232.
32. Ogiwara,H., Ui,A., Onoda,F., Tada,S., Enomoto,T. and Seki,M. (2006) Dpb11, the budding yeast homolog of TopBP1, functions with the checkpoint clamp in recombination repair. *Nucleic Acids Res*., **34**, 3389–3398.
33. White,C.I. and Haber,J.E. (1990) Intermediates of recombination during mating type switching in *Saccharomyces cerevisiae*. *EMBO J*., **9**, 663–673.
34. Koy,J.F., Pleninger,P., Wall,L., Pramanik,A., Martinez,M. and Moore,C.W. (1995) Genetic changes and bioassays in bleomycin- and phleomycin-treated cells and their relationship to chromosomal breaks. *Mutat. Res*., **336**, 19–27.
35. Moore,C.W. (1988) Internucleosomal cleavage and chromosomal degradation by bleomycin and phleomycin in yeast. *Cancer Res*., **23**, 6837–6843.
36. Wang,X., Ira,G., Tercero,J.A., Holmes,A.M., Diffley,J.F. and Haber,J.E. (2004) Role of DNA replication proteins in double-strand break-induced recombination in *Saccharomyces cerevisiae*. *Mol. Cell. Biol*., **16**, 6891–6899.
37. Van Dyck,E., Stasiak,A.Z., Stasiak,A. and West,S.C. (1999) Binding of double-strand breaks in DNA by human Rad52 protein. *Nature*, **398**, 728–731.
38. Hiom,K. (1999) DNA repair: Rad52-the means to an end. *Curr. Biol*., **9**, 446–448.
39. Lundblad,V. (2000) DNA ends: maintenance of chromosome termini versus repair of double strand breaks. *Mutat. Res*., **451**, 227–240.
40. Valencia,M., Bentele,M., Vaze,M.B., Herrmann,G., Kraus,E., Lee,S.E., Schar,P. and Haber,J.E. (2001) NEJ1 controls non-homologous end joining in *Saccharomyces cerevisiae*. *Nature*, **414**, 666–669.
41. Van Attikum,H., Fritsch,O., Hohn,B. and Gasser,S.M. (2004) Recruitment of the INO80 complex by H2A phosphorylation links ATP-dependent chromatin remodeling with DNA double-strand break repair. *Cell*, **119**, 777–788.
42. Haber,J.E. (2002) Switching of *Saccharomyces cerevisiae* mating-type genes. In Craig,N.L, Craigie,R., Gellert,M. and Lambowitz,A.M. (eds), *Mobile DNA II*. ASM Press, Washington, DC, pp. 927–952.
43. Holmes,A.M. and Haber,J.E. (1999) Double-strand break repair in yeast requires both leading and lagging strand DNA polymerases. *Cell*, **96**, 415–424.
44. Michel,B., Flores,M.J., Viguera,E., Grompone,G., Seigneur,M. and Bidnenko,V. (2001) Rescue of arrested replication forks by homologous recombination. *Proc. Natl Acad. Sci. USA*, **98**, 8181–8188.
45. Rothstein,R., Michel,B. and Gangloff,S. (2000) Replication fork pausing and recombination or 'gimme a break'. *Genes Dev*., **14**, 1–10.
46. Lisby,M., Barlow,J.H., Burgess,R.C. and Rothstein,R. (2004) Choreography of the DNA damage response spatiotemporal relationships among checkpoint and repair proteins. *Cell*, **118**, 699–713.
47. Paques,F. and Haber,J.E. (1999) Multiple pathways of recombination induced by double-strand breaks in *Saccharomyces cerevisiae*. *Microbiol. Mol. Biol. Rev*., **63**, 349–404.
48. Ivanov,E.L. and Haber,J.E. (1995) RAD1 and RAD10, but not other excision repair genes, are required for double-strand break-induced recombination in *Saccharomyces cerevisiae*. *Mol. Cell. Biol*., **15**, 2245–2251.
49. Sugawara,N., Paques,F., Colaiacovo,M. and Haber,J.E. (1997) Role of *Saccharomyces cerevisiae* Msh2 and Msh3 repair proteins in double-strand break-induced recombination. *Proc. Natl Acad. Sci. USA*, **94**, 9214–9219.
50. Gangloff,S., Soustelle,C. and Fabre,F. (2000) Homologous recombination is responsible for cell death in the absence of the Sgs1 and Srs2 helicases. *Nature Genet*., **25**, 192–194.
51. Onoda,F., Seki,M., Miyajima,A. and Enomoto,T. (2000) Elevation of sister chromatid exchange in *Saccharomyces cerevisiae* sgs1 disruptants and the relevance of the disruptants as a system to evaluate mutations in Bloom's syndrome gene. *Mutat. Res*., **459**, 203–209.
52. Jenne,D.E., Tinschert,S., Stegmann,E., Reimann,H., Nurnberg,P., Horn,D., Naumann,I., Buske,A. and Thiel,G. (2000) A common set of at least 11 functional genes is lost in the majority of NF1 patients with gross deletions. *Genomics*, **66**, 93–97.